ISSN No.: 2455-6130
Volume 1, Issue 4, 2016, pp. 16-28

website: www.ijoetr.com

International Journal of Emerging Trends in Research

Practical investigation of a single pass triangular shaped duct solar air heater having v-shaped ribs on the absorber plate

Bikas Prasad
Department of Mechanical Engineering SITE, Meerut, SVSU Meerut (U.P),India

Abstract

Conventional sources of energy are depleting very fast due to increase in the needs of people. So there is a need to develop an alternating method to fulfil these ever increasing needs of energy. Earlier experimental studies on single pass solar air heaters having roughened duct have revealed that the heat transfer coefficient is generally higher depending upon the type of roughness on the absorber plate. There is no experimental study available in the literature for Single pass solar air heater having triangular duct with roughened absorber plate. This topic has been taken to see the effect of artificial roughness on the absorber plate and the importance of Single pass solar air heater on the friction factor and heat transfer characteristics.

Keywords: solar; air heater; duct; ribs

1. Introduction

Energy plays a very crucial role in the life of every one either it is the matter of economic growth or the growth of industrialization [1]. Energy is the basic need of life. Classical energy resources are limited and their reserves are threatened due to the huge demand for energy. There is a need of switching over to non-conventional energy source like solar energy, wind energy, tidal energy etc. which are non-exhaustible types of energy sources and produce no pollution. The percentage use of various sources of energy consumed by the world is given in Table 1[2].

More over modern sources of energy such as nuclear energy may form a threat to the environment and world safety. Because the main source of nuclear power are radioactive materials and the radiation is hazardous to both for nature and for living things. Therefore additional sources of energy are required, which are cheap, safe and environmentally compatible

Table 1 Percentage use of sources consumed by world

S. No.	Energy Sources	Percentage Utilization
1.	Oil	38.3%
2.	Coal	32.5%
3.	Gas	19%
4.	Wood	6.6%
5.	Hydro	2.0%
6.	Dung	1.2%
7.	Waste	0.3%
8.	Uranium	0.13%

Scientific definition of energy is the capacity to do work. However, energy is the basic ingredient needed to sustain life and development because it is needed in various forms to fulfil day to day requirements. Social, cultural and economic development of the people is determined to a large extent by the amount of per capita energy consumed and by the effectiveness of the technological means with which it is put to work. Man has needed and used energy at an increasing rate for his development and well being ever since he came on the earth a few million years ago, the requirement, need of energy as well as availability and consumption has changed eventually from generation to generation like primitive man required energy primarily in the form of food and it becomes available for him in the form of plants or animals which he hunted, subsequently he discovered fire and his energy needs increased as he started to make use of wood and other biomass to supply the energy. As the civilization moved further the prospective of man's need & requirement of energy brought lot of options for him as he added a new dimension to the use of energy by domesticating and training animals, also he began to use wind for sailing ships and wind for driving windmills and the force of falling water to turn the water wheels. The energy resources may also be classified as non-renewable and renewable energy resources. Non-renewable energy resources like coal, oil, gas have been formed over very long period of time in nature and are likely to be exhausted in mere decades or centuries. Renewable energy resources are of many types like:

1. Solar Energy 2.Wind Energy 3. Hydropower Energy 4. Biomass Energy 5. Tidal Energy 6. Geothermal Energy

Among all the alternative of renewable energy resources, the sun is of domineering nature. The solar radiation striking the earth surface is absorbed by the earth and used for further energy generation. Solar energy is one of the most important alternatives for energy generation in future because the total energy we receive from the sun is around 35000 times the total energy used by man [3]. The average intensity of solar radiation in India works out to be approximately 2000 kWh/m^2 [4] as compared to the world average of 2500 kWh/m^2. The major drawback with this resource is its low intensity and it is erratic in nature. The solar intensity reaching the earth is typically about 1 kW/m^2, however availability varies with location and time [3]. In spite of these limitations, solar energy appears to be the most promising among all the renewable energy resources.

2. Literature review

In this section, an extensive review of literature in the area of solar energy collection system, with special reference to artificial roughness on absorber plate is being presented. It has been brought out that there are several schemes that can be implemented to enhance the thermal performance of this most commonly employed energy collection devices. These methods along with their enhancement potential have been discussed in this chapter.

2.1 Categorization of literature

Literature is divided into following categories:

- Concept of artificial roughness
- Flow pattern
- Roughness geometries used in solar air heater ducts
- Thermal efficiency of solar air heater
- Effective efficiency of solar air heater

3. Experimental methodology

A schematic view of the experimental set-up has been shown in Figure 1. The experimental set-up consists of a single pass triangular channel, plenum, and electric heater, pressure measuring devices, temperature measuring devices and blower. A single pass triangular channel has been designed and fabricated to see the effect of artificial roughness used in single pass Heat exchanger. The experimental set-up consists of a triangular channel which has been designed and fabricated from wood. The dimensions of the triangular channel are 2010 mm × 180 mm × 48 mm. The entry section has been designed according to ASHARE standards i.e. $5\sqrt{WH}$ [34]. Test section is of 1600 mm and 500 mm of gap is provided after test section for the proper circulation of air.

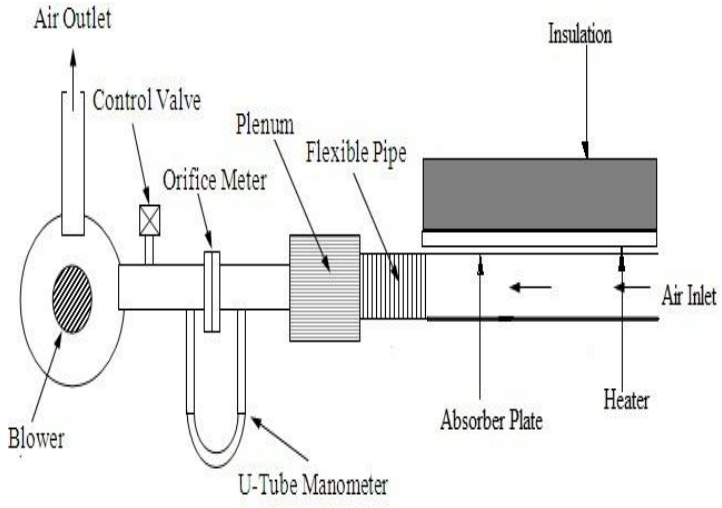

Figure 1 A schematic view of experimental set up

The atmospheric air is sucked by the means of a blower having capacity of 3 HP through the inlet portion of the single pass triangular channel. The air moves to the outlet of the triangular channel through the triangular duct. The exit section of the channel is connected to a GI pipe via rectangular mixing chamber called plenum. The mass flow rate of the air has been measured with the help of a calibrated orifice plate provided in the GI pipe. The pressure drop across the orifice plate has been measured with the help of a U-tube manometer.

The test section is of galvanized iron which acts as an absorber plate. The roughness is created on the upper and lower part of the absorber plate with the help of ribs. A heater is used to provide the constant heat flux to the absorber plate The temperatures of the heated absorber plate and air are measured by the help of copper-constantan thermocouples and a digital micro-voltmeter. The pressure drop across the test section has been measured with the help of a micro-manometer. Two control valves are provided to control the mass flow rate of the air at the exit and entrance of the blower. The full description of the major components of the experimental set-up is given below:

3.1 Roughness geometry and range of parameters

V shaped ribs are fixed on one side of the absorber plate with the help of glue. The ribs are attached to absorber plate forming V-shape. The pitch and the height of ribs are given in non-dimensional form expressed as relative roughness height (e/D_h) and relative roughness pitch (p/e). The inclination of the ribs is expressed as angle of attack (α). The range of parameters is given in Table 2.

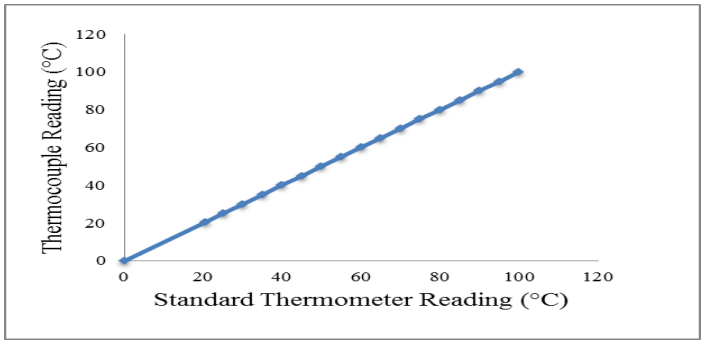

Figure 2 Calibration curve for thermocouples

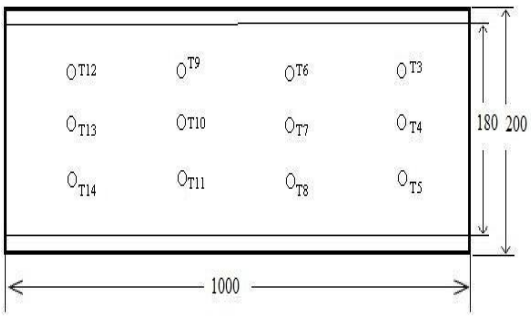

Figure 3 Location of the thermocouples on the absorber plate

Table 2 Range of parameters

S. No.	Parameter	Range
1.	Aspect ratio (W/H)	3.4
2.	Relative roughness height (e/D_h)	0.044
3.	Relative roughness pitch (p/e)	4-16
4.	Angle of attack (α)	60°
5.	Reynolds number	2300-17000

3.2 Experimental steps

Before starting the experimentation it is necessary to check that there should be no leakage. If there is any leakage do the proper arrangement to stop that leakage. Check all the instruments properly.

The experimental runs were conducted under quasi-steady state to collect the relevant data for heat transfer and friction factor. The setup was allowed to attain quasi-steady state before the data was recorded at different mass flow rates. The following data were recorded:

1. Air temperature at different points on the duct and the temperature of absorber plate at 12 different locations on the absorber plate.
2. Pressure drop across the test section.
3. Pressure measurement across the orifice meter.

3.3 Data reduction

The raw experimental data have been reduced to obtain the average plate temperature, average air temperature, mass flow rate and Reynolds number. These data were then used to determine the heat transfer coefficient, Nusselt number and friction factor. Relevant expressions for the computation of above mentioned parameters and some intermediate parameters have been given below;

3.3.1 Mean Plate and Air Temperature

The mean plate temperature T_p is calculated by the average of the temperatures recorded at various locations on the absorber plate as shown in Figure 3 and is given as;

$$T_p = \frac{T_3 + T_4 + T_5 + T_6 + T_7 + T_8 + T_9 + T_{10} + T_{11} + T_{12} + T_{13} + T_{14}}{12} \qquad (1)$$

The bulk mean air temperature, T_f is the arithmetic mean of the measured values of air temperature at the entry and exit to the test section,

$$T_f = \frac{T_1 + T_2}{2} \qquad (2)$$

3.3.2 Mass Flow Rate of Air

Mass flow rate of air has been determined by the pressure drop measured across the calibrated orifice meter using the following expression.

$$m = C_d A_O \sqrt{\frac{2\rho(\Delta P_O)}{1-\beta^4}} \quad (3)$$

3.3.3 Velocity of Air through Duct

The velocity of air is calculated from the knowledge of mass flow rate and area of flow i.e the cross section area of the duct as,

$$V = \frac{m}{\rho WH} \quad (4)$$

3.3.4 Hydraulic Diameter

The hydraulic diameter of the triangular section of the duct is determined from the relationship as given below,

$$D_h = \frac{4A_c}{P} \quad (5)$$

3.3.5 Reynolds Number (Re)

The Re of airflow in the duct is calculated from the following relationship:

$$\mathrm{Re} = \frac{\rho V D_h}{\mu} \quad (6)$$

3.3.6 Friction Factor (f)

Pressure drop (ΔP) measured across the test section length is used to find out the friction factor using Darcy Wiesbach equation as below:

$$f = \frac{2(\Delta P_{duct})D_h}{4\rho L V^2} \quad (7)$$

3.3.7 Heat Transfer Coefficient (h)

The heat transfer coefficient is calculated from the relationship given below;

$$h = \frac{Q_u}{A_p(T_p - T_f)} \quad (8)$$

where T_p and T_f are the mean absorber plate and the fluid temperatures respectively, as discussed above and

Heat transfer rate (Q_u) to the air is given by

$$Q_u = mC_p(T_O - T_i) \quad (9)$$

3.3.8 Nusselt Number (Nu)

The heat transfer coefficient calculated using equation 3.8 is used to determine the Nusselt number as given below;

$$Nu = \frac{hD_h}{k} \quad (10)$$

4. Result and discussion

When the fluid enters into the duct and comes in contact with wall, the layer in contact with wall comes to rest. And due to friction the fluid particles in the adjacent layer slowdowns. To make up this velocity reduction, the velocity of the fluid at the midsection of the triangular duct has to increase to keep the mass flow rate through the rectangular duct constant. As a result, velocity gradient develops along the channel. The flow becomes turbulent because of roughness provided above and underside of absorber plate due to reattachment point or laminar sub-layer breakup.

As pointed earlier the thermal performance of solar air heater can be enhanced by providing artificial roughness on the absorber plate. However, this also brings about a substantial increase in pumping power and thus it becomes important to select the roughness geometry in such a way that it will improve the heat transfer while keeping the value of the increased pumping power at minimum possible level. This chapter has been devoted to show the behavior Nusselt number and friction factor with different roughness parameters and operating parameters like, relative roughness pitch (P/e), relative gap position (d/w), and Reynolds number have been shown on the heat transfer and friction factor. Roughened solar air heater duct has also been compared to smooth one.

4.2 Nusselt number (Nu)

The values of Nusselt number for different orientation of roughness geometry in double pass solar air heater were computed on the basis of experimental data for different roughness and operating parameters and plotted as a function of Reynolds number. The Nusselt number increases monotonously with an increase in Reynolds number i.e. Nusselt number varies directly with Reynolds number due to increase in swirl intensity caused by increase in turbulent kinetic energy and turbulent dissipation rate with the increase in Reynolds number. But the maximum value of the Nusselt number occur at relative roughness height of (e/D_h) 0.043, relative roughness pitch (p/e) of 8 and angle of attack (α) of 60° respectively. Discussion of effect of various roughness parameters and operating parameter on heat transfer is given below.

4.2.1 Effect of Relative Roughness Pitch (P/e)

Figure 4 shows the effect of Reynolds number on Nusselt number for various relative roughness pitch (p/e) values varies from 4-16 and for a fixed value of angle of attack (α) and a fixed value of relative roughness height (e/D_h) of 60° and 0.044 respectively. The graph has been plotted to compare the Nusselt number for a single pass solar air duct having V-shape rib roughness

element on the absorber plate for different values of relative roughness pitch (P/e). Figure 4 shows that Nusselt number increases with the increase in Reynolds number for different values of relative roughness pitch (p/e). From Figure 4 it is clear that the maximum value of Nusselt number has been found corresponding to relative roughness pitch of 8.

As the value of relative roughness pitch (p/e) goes on increasing the number of reattachment points on the surface get decreased due to which less heat transfer take place as reported by Verma and Prasad .So, the maximum heat transfer occur when reattachment points are maximum on surface, hence maximum heat transfer occur at relative roughness pitch (p/e) value of 8. The flow gets separated while being upstream of a rib but does not get reattached if the relative roughness pitch (p/e) is less than 8. Figure 5 shows the variation of Nusselt number as a function of relative roughness pitch (p/e) for different values of Reynolds number and for fixed value of relative roughness height (e/D_h) and angle of attack (α).

Effect of Relative Gap Position (d/w)

Fig 6 shows the variation of Nu with Re at different values of d/w. The other roughness parameters were kept as P/e = 8, α= 60˚, g/e=1and e/D_h=0.043. At all Re, the value of Nu is more for discrete V-down rib than that for continuous V-down rib. This is because gap in continuous rib results in enhancement of local Nu at the downstream side of the gap thereby causing increase in average Nu. This local Nu enhancement is caused by increased flow-mixing and turbulence resulting from accelerated flow through the gap. To clearly show the variation of Nu with d/w, the result are re-plotted in Fig. 5 for different Re. The Nu increases for d/w increase from 0.20 to 0.65 and then decreases as the d/w is increased from 0.60 to 0.80. For V-down rib, the local Nu in span-wise direction between adjacent ribs reduces from leading edges to the V-apex due to increase in boundary layer thickness and with the creation of gap in the rib, a region of high local Nu develops downstream of the gap. Therefore, depending upon the position of the gaps, the average Nu varies. If the gaps are created towards the V-apex region, it will help in increasing the local Nu in the low Nu region and hence the average Nu is enhanced. It is seen that this happens till the d/w of 0.60. It is anticipated that if the gaps are placed too close to the V-apex, the two high Nu regions generated downstream of the gap in both legs of V-rib may overlap, and therefore will not cause comparable effect of increase in the average Nu i.e., providing the gaps nearer to the V-apex (d/w > 0.60) results in lesser increase in

average Nu. These results broadly agree with earlier studies on inclined ribs with gap who have also reported the existence of optimum gap position.. The trend of variation in Nu with d/w remains same for all P/e values. The maximum Nu occurs at d/w of 0.65 for all P/e values.

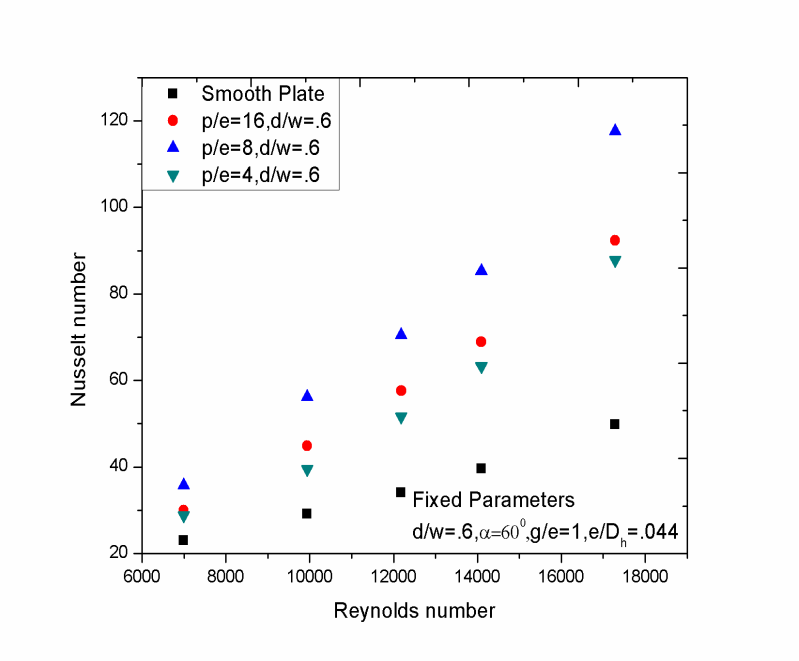

Figure 4 Variation of the Nusselt number with the Reynolds number for different values of P/e and for fixed $e/D_h = 0.044$ and $\alpha = 60°$

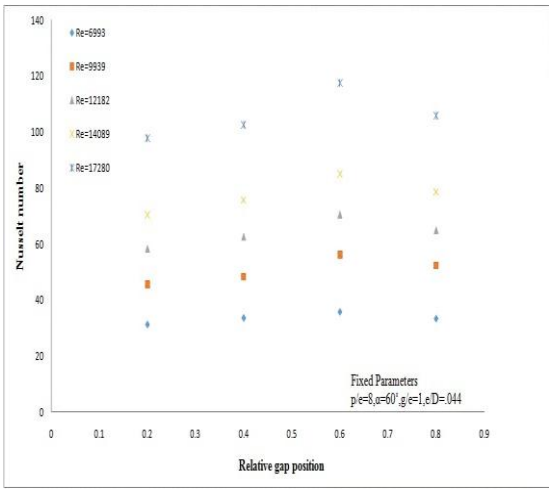

Figure 5 Variation of Nusselt number with relative gap position (d/w) at different Reynolds number.

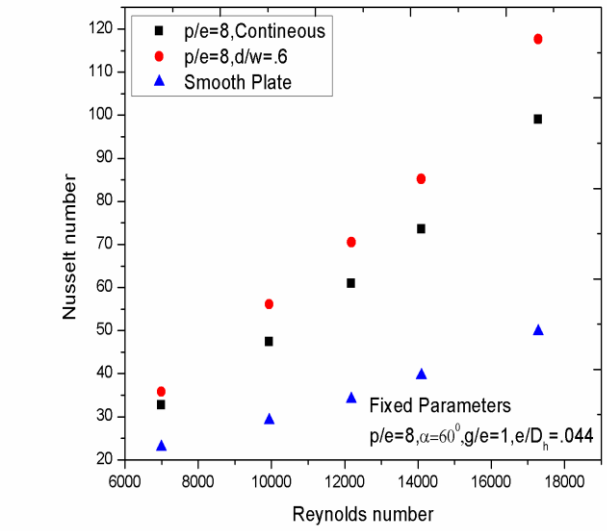

Figure 6 Variation of Nusselt number with Reynolds number for discrete V-down ribbed duct, continuous V-down ribbed duct and smooth duct.

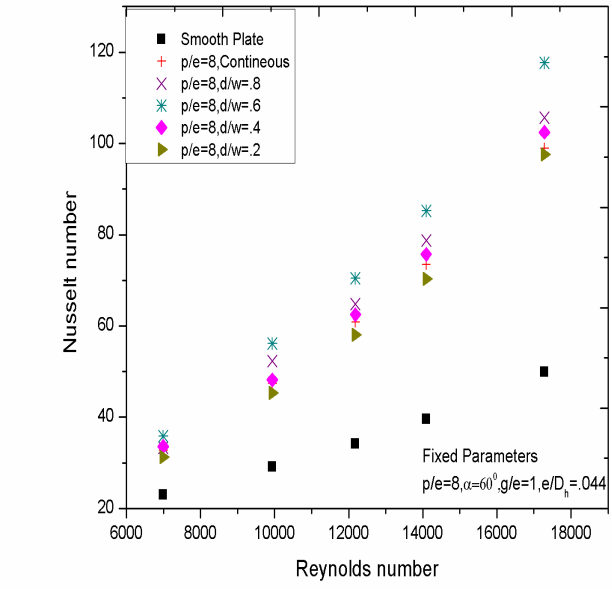

Figure 7 Variation of Nusselt number with Reynolds number at different relative gap position (d/w)

4.2.2 Friction Factor (f)

The friction factor (f) obtained from the experimentation have been plotted as a function of Reynolds number having different orientation of roughness geometry. The friction factor decreases with the increase in the Reynolds number. But the maximum value of the friction factor occur at relative roughness height of (e/D_h) 0.044, relative roughness pitch (p/e) of 10 and angle

of attack (α) of 60° respectively. Discussion of effect of various roughness parameter and operating parameter on heat transfer is given below.

4.2.3 Effect of Relative Roughness Pitch (p/e)

Figure 8 shows the effect of relative roughness pitch (p/e) values varies from 4-16 on friction factor with Reynolds number for a fixed value of angle of attack (α) and relative roughness height (e/D_h) of 60° and 0.044 respectively. The maximum value of friction factor occurs at relative roughness pitch (p/e) of 8. In Figure 4.8 the variation of friction factor with Reynolds number is shown and we get from the graph that with the increase in Reynolds number the Friction factor decreases linearly for all values of Relative roughness pitch (p/e).

Also in Figure 9 the value of Friction factor with respect to Relative roughness height (p/e) for different Reynolds number is shown.

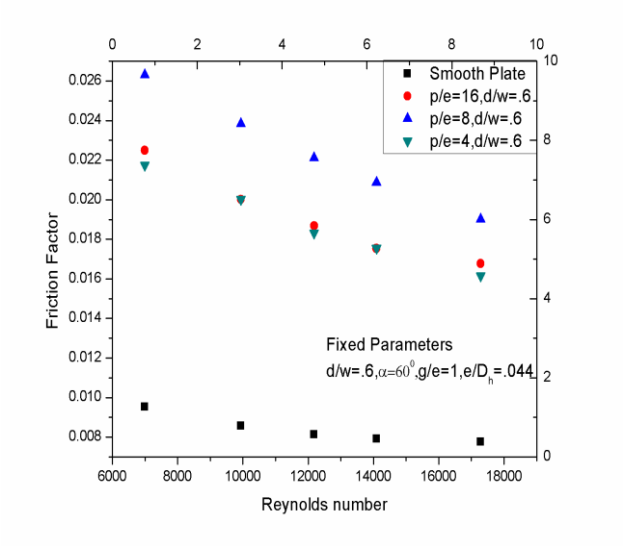

Figure 8 Variation of friction factor with the Reynolds number for different values of P/e and for fixed e/D_h =0.044 and α =60°

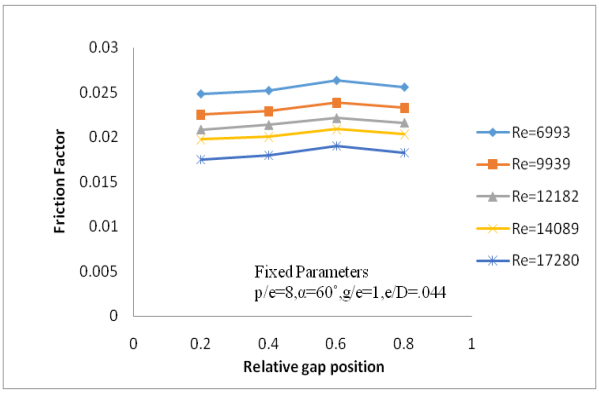

Figure 9 Variation of frictional factor with relative gap position (d/w) at different Reynolds number

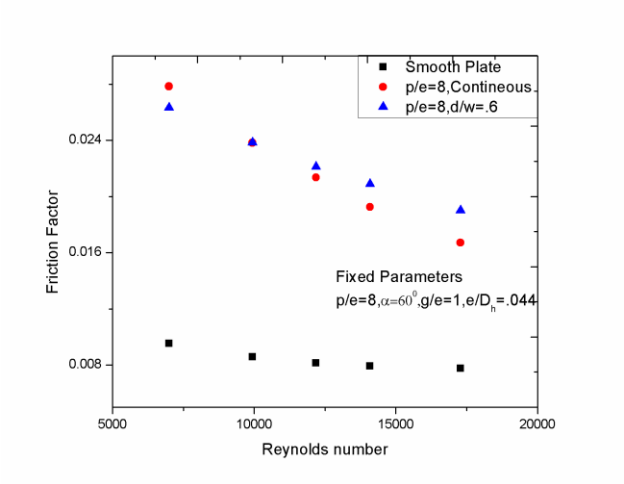

Figure 10 Variation of Frictional factor with Reynolds number for discrete V-down ribbed duct, continuous V-down ribbed duct and smooth duct.

5. Conclusions

In this analysis a variety of values for various operating and governing parameters were selected and then the calculations were made to check the values of thermal efficiency and effective efficiency. So on the basis of the above calculated data following conclusions can be drawn.

1. The heat transfer coefficient and the friction factor get enhanced by providing the artificial roughness on low side of the absorber plate in the Triangular Single pass solar air heater duct.
2. The maximum heat transfer and the friction factor occur at the relative roughness pitch (p/e) of 8 and relative angle of attack (α) of 60° for the fixed value of relative roughness height (e/D_h) of 0.044 And relative gap position of (d/w) of 0.6.
3. The correlations for the Nusselt number and the friction factor have been derived. The deviation between the experimental value of Nusselt number and predicted value of Nusselt number found to be ±15%. The deviation between the experimental value of friction factor and predicted value of friction factor found to be ±14%.
4. The maximum thermal and thermo hydraulic efficiency occur at the relative roughness pitch (p/e) of 8 and relative angle of attack (α) of 60° for the fixed value of relative roughness height (e/D_h) of 0.044 and (d/w) of 0.6.
5. Maximum heat transfer occurs at the relative gap position of 0.6 and maximum frictional factor also corresponds to same value of relative gap position (d/w)

References

[1] G.D.Rai, Non-Conventional energy sources, Khanna publications, New Delhi, 1997

[2] G.K.Ghosh, Soalr energy, The infinite source, Ashish publishing house, New Delhi 1991.

[3] Ministry of New and Renewable Energy, Government of India, http://www.mnes.nic.in.

[4] Goswami, D.Y., Kreith, F. and Kreider, J.K., Principles of Solar Engineering, Taylor and Francis, 2003.

[5] Sen, Z. Energy and Climate Change, Solar energy fundamentals and modeling techniques, Verlag London limited: Springer; 2008.

[6] Duffie and Beckman, Soalr engineering of thermal processes (second edition), A Wiley Inter science publication, John Wiley and sons, Inc., Newyork, 1980

[7] Garg, H.P. and Prakash, J.P., Solar Energy- Fundamentals and Applications, Tata McGraw-Hill, New Delhi.

[8] Satcunanathan, S. and Deonarine, S., A two pass solar air heater, Solar Energy 15(1) (1973), 41-49.

[9] Malhotra, A., Garg, H.P. and Rani, U., The effect of gap spacing on convective losses in flat plate collectors, Proceeding of National Solar Energy Convection, I.I.T Bombay (1979), 52-56.

[10] Malhotra, A., Garg, H.P. and Rani, U., Minimizing convective heat losses in flat plate solar collectors, Solar Energy 25(6) (1980), 521-526.

[11] Bevill, V.D. and Brandt, H., A solar energy collector for heating air, Solar Energy 12 (1968), 19-29.

[12] Saini, J.S., Artificial roughness- A potential method of enhancement of efficiency of solar air heater, National conference on Emerging Energy Technologies (NCEET-2003), NIT Hamirpur,2003.

[13] Gautam, V., Singh, R. P., Kataria, R., & Kumar, J. (2016). A Critical Review on the Impact of Input Factors on Process Outcomes in Drilling of Aluminium Alloys. International Journal of Emerging Trends in Research, 1(1), 12-18.

[14] Sharma, P., & Singhal, S. (2016). Design and evaluation of layout alternatives to enhance the performance of industry. *OPSEARCH*, 1-20.

[15] Kataria, R., Kumar, J., & Pabla, B. S. (2016) A review on ultrasonic machining. International Journal of Emerging Trends in Research, 1(2), 24-34.

[16] Bopche S.B., Tandale M.S., "Experimental Investigation on Heat Transfer and Friction Characteristics of a Turbulator Roughened Solar Air Heater Duct", International Journal of Heat and Mass Transfer, 2009, vol.52, pp.2834-2848.

[17] Cortes A, Piacentini R, "Improvement of the Efficiency of a Bare Solar Collector by Means of Turbulence Promoters", Applied Energy, 1990, vol.36, pp.253–6.

[18] Jaurker A.R., Saini J.S., Gandhi B.K., "Heat Transfer and Friction Characteristics of Rectangular Solar Air Heater Duct Using Rib Grooved Artificial Roughness", Solar Energy, 2006, vol.80, pp.895-907.